

Stochastic modeling and survival analysis of marginally trapped neutrons for a magnetic trapping neutron lifetime experiment

K. J. Coakley^{a,*}, M. S. Dewey^b, M. G. Huber^b, P. R. Huffman^{c,d}, C. R. Huffer^{c,d}, D. E. Marley^{b,c}, H. P. Mumm^b, C. M. O'Shaughnessy^{e,d}, K. W. Schelhammer^{c,d}, A. K. Thompson^b, A. T. Yue^b

^a*National Institute of Standards and Technology, 325 Broadway, Boulder, CO 80305*

^b*National Institute of Standards and Technology, 100 Bureau Drive, Stop 8461, Gaithersburg, MD 20899*

^c*North Carolina State University, 2401 Stinson Drive, Box 8202, Raleigh, NC 27695*

^d*Triangle Universities Nuclear Laboratory, 116 Science Drive, Box 90308, Durham, NC 27708*

^e*University of North Carolina at Chapel Hill, 120 E. Cameron Ave., CB #3255, Chapel Hill, NC 27599*

Abstract

In a variety of neutron lifetime experiments, in addition to β -decay, neutrons can be lost by other mechanisms including wall losses. Failure to account for these other loss mechanisms produces systematic measurement error and associated systematic uncertainties in neutron lifetime measurements. In this work, we construct a competing risks survival analysis model to account for losses due to the joint effect of β -decay losses, wall losses of marginally trapped neutrons, and an additional absorption mechanism. We determine the survival probability function associated with the wall loss mechanism by a Monte Carlo method. We track marginally trapped neutrons with a symplectic integration method that assumes neutrons are classical particles. We model wall loss probabilities of Ultracold Neutrons (UCNs) that collide with trap boundaries with a quantum optical model. Based on a fit of the competing risks model to a subset of the NIST experimental data, we determine the mean lifetime of trapped neutrons to be approximately 700 s – consid-

*Corresponding author

Email address: kevincoakley@nist.gov (K. J. Coakley)

erably less than the current best estimate of (880.1 ± 1.1) s promulgated by the Particle Data Group [1]. Currently, experimental studies are underway to determine if this discrepancy can be explained by neutron capture by ^3He impurities in the trapping volume. We also quantify uncertainties associated with Monte Carlo sampling variability and imperfect knowledge of physical models for neutron interactions with materials at the walls of trap as well as beam divergence effects. Finally, in a Monte Carlo experiment, we demonstrate that when the trapping potential is ramped down and then back up again, systematic error due to wall losses of marginally trapped neutrons can be suppressed to a very low level. Monte Carlo simulation studies indicate that this ramping strategy is more efficient than an alternative ramping scheme where UCNs are produced when the field is fully ramped, and then increased to its maximum value after the trap is filled. The survival probability formalism developed here should be applicable to other experiments where neutron (or other particle) loss mechanisms are non-trivial (i.e., where the associated survival probability function with the loss mechanism is non-exponential).

Keywords: Chaotic scattering

Competing risks, Magnetic trapping, Marginally trapped neutrons, Monte Carlo simulation, Neutron lifetime, Stochastic modeling, Survival analysis, Symplectic integration

PACS: code 81.07.Gf, 07.05.Kf, 07.79.-v, 07.79.Lh

1. Introduction

According to the Particle Data Group, the current best estimate of the mean lifetime of the neutron τ_n is (880.1 ± 1.1) s [1]. This uncertainty is largely due to systematic effects. Hence, reduction of systematic uncertainties is key to reducing the overall uncertainty of the mean lifetime of the neutron [2]. To emphasize this point, we note that the difference between neutron lifetime estimates determined by beam and bottle experiments is (8.4 ± 2.2) s. This difference is likely due to unresolved systematic errors [3]. In trapping experiments, marginally trapped neutrons can escape a trapping volume before they β -decay. Failure to account for this loss mechanism leads to systematic measurement error and associated systematic uncertainties in neutron lifetime measurements [4-9]. In this work, we focus on wall losses of marginally trapped Ultracold Neutrons (UCNs) in a magnetic trap-

ping experiment at NIST. Since the probability of losing a neutron when it interacts with materials at a wall depends, in part, on neutron energy, the survival probability of a marginally trapped UCN is non-exponential. We estimate the systematic error in the neutron lifetime estimate due to marginally trapped UCNs for a particular subset of the NIST data where the trapping potential is static. We stress that systematic error (and associated systematic uncertainty) associated with marginally trapped UCNs can be reduced by field ramping strategies to very low levels with the cost of increasing random uncertainty. Hence, the systematic error we report for the static potential case does not apply to cases where marginally trapped UCNs are purged by field ramping methods.

In the NIST experiment [5,6] an UCN is produced during a trap-filling stage when a 12 K neutron is scattered to near rest in liquid helium by single phonon emission [10]. After filling the trap and blocking the cold beam that produces UCNs, light produced by neutron decay and background events is detected by a pair of phototubes. A marginally trapped (or above threshold) neutron is an UCN with sufficient energy to escape the trap by interacting with materials at the boundary of the trap [11,12,13]. A UCN with insufficient energy to escape the trap by the wall loss mechanism is a below threshold UCN. Since a marginally trapped UCN can be lost to the walls before it β -decays, the decay rate of marginally trapped UCNs is not exponential. Hence, when wall losses are non-negligible, on average, the observed β -decay rate of neutrons is also non-exponential. Thus, if one were to fit an exponential model to such decay event data, one would expect the associated estimate of the neutron lifetime to be biased.

Here, we develop a competing risks survival analysis model [14,15,16,17] that accounts for loss of UCNs due to β -decay, wall losses, upscattering and other absorption mechanisms. Determination of the survival probability function associated with the wall loss mechanism is the key problem addressed by this work. We determine the survival probability function associated with wall losses by a Monte Carlo method as described in [18].

Based on the conditional survival probability function of an UCN that survives the filling stage, we construct a prediction model for observed data. If β -decay and wall losses were the only loss mechanisms, and we had perfect knowledge of the survival probability of marginally trapped UCNs as well as possible backgrounds, a fit of this model to data would yield a nearly unbiased estimate of the true neutron lifetime given a sufficient amount of data. In practice, there are other loss mechanisms including upscattering

and neutron absorption by ^3He that affect the mean lifetime of neutrons in the trap. Still, given perfect knowledge of the survival probability functions associated with these loss mechanisms, one could correct the measured neutron lifetime of trapped UCNs and recover the true neutron lifetime in an ideal noise-free experiment. We analyze a subset of the NIST experimental data where neutrons are confined in a static potential to quantify various sources of systematic measurement error and associated uncertainty. For the data analyzed, the measured lifetime of trapped UCNs is approximately 700 s. We attribute the discrepancy between our estimate and the current best estimate of 880.1 s to an additional absorption loss mechanism. Currently, experiments are underway to determine if ^3He impurities are sufficiently high to explain the discrepancy.

In some runs of the NIST experiment, we vary the trapping potential to purge marginally trapped UCNs. In a simulation experiment, we demonstrate that field ramping can in principle reduce systematic measurement error and associated uncertainty due to marginally trapped UCNs to very low levels at the expense of purging below threshold UCNs. For a particular example, we demonstrate that the above ramping strategy is more efficient than one where neutrons are trapped when the field is fully ramped and then increased to its maximum value. By more efficient, we mean that the expected number of below threshold UCNs after ramping is higher for our ramping strategy as compared to the alternative strategy given that both methods purge marginally trapped UCNs with nearly the same efficiency.

In this paper, we first present our physical and computational methods for simulating UCN trajectories and loss probabilities of UCNs due to wall interactions. Next, we develop our competing risks survival analysis model and apply it to experimental data acquired at NIST. We also quantify uncertainties associated with Monte Carlo sampling variability and imperfect knowledge of physical models for neutron interactions with materials at the walls of trap and beam divergence effects. Finally, in a Monte Carlo simulation experiment, we demonstrate that field ramping can reduce systematic error due to wall losses of UCN to a very low level at the expense of reducing the expected number of trapped UCNs after ramping.

2. Physical model

2.1. Trapping potential model

In the NIST experiment, an UCN with sufficiently low energy is trapped in the potential field produced by the interaction of the magnetic moment of a neutron and a spatially varying magnetic field (Figure 1) and gravity. For tracking UCNs in the trapping volume, assuming adiabatic spin transport, the potential is

$$V(\mathbf{x}) = \mu|\mathbf{B}(\mathbf{x})| + m_n g y, \quad (1)$$

where \mathbf{B} is the magnetic field, m_n and μ are the mass and magnetic moment of the neutron respectively, $\mathbf{x} = (x, y, z)$ is spatial location of the neutron in the Cartesian coordinates shown in Figure 1, and g is the acceleration due to gravity.

We define a nominal trapping volume corresponding to $-z_o \leq z \leq z_o$ where z is the axial coordinate and $z_o = 37.5$ cm (see Figure 1). An UCN with total energy (kinetic plus potential) greater than the minimum of the potential V_{\min} on the boundary of the nominal trapping volume is defined to be a marginally trapped (or above threshold) UCN. An UCN with energy less than or equal to V_{\min} is a below threshold UCN. We stress that there is not a physical boundary at $z = -37.5$ cm. However, as shown in Figure 1, as z is reduced from $z \approx -37.5$ cm to -60 cm, the trapping potential decreases dramatically. For modeling purposes and to speed up Monte Carlo simulations, it is important to define a nominal trapping volume so that all UCN with initial energy less than the minimum value trapping potential on the boundary of the nominal trapping volume never interact with materials at the ZZ at $z = -60$ cm and $z = 37.5$ cm, nor the cylindrical boundary $r = 5.6$ cm. If we choose the lower axial boundary to be much less than -37.5 cm, this condition is violated. Different choices of the minimum axial location of the nominal trapping volume affect results. In Section 4.3, we quantify this effect. For a typical static trap configuration of the NIST experiment, $V_{\min} = 139$ neV. We assume that probability distribution function of the initial speed $|v|$ of an UCN produced in the trap has a quadratic form [18,19] $f(|v|) \propto |v|^2$ for low velocities of interest.

We determine a neutron trajectory based on its initial position and momentum, by solving the classical equations of motion

$$\dot{\mathbf{p}} = F(\mathbf{x}) = -\nabla V(\mathbf{x}), \quad (2)$$

and

$$\dot{\mathbf{x}} = \frac{\mathbf{p}}{m_n}, \quad (3)$$

with an optimal fourth order symplectic integration scheme [18,19,20,21]. We predict $|\mathbf{B}|$ at arbitrary points in the trapping volume with a three-dimensional tensor-product spline interpolant [22] where the order of the spline is four in each direction. We determine the tensor-product B-spline coefficients from values of $|\mathbf{B}|$ computed on a grid by a code that solves the Biot-Savart law numerically based on the geometry of the solenoid and current bars that produce the magnetic field. With this tensor-product method, we evaluate the potential and its gradient at arbitrary locations within the trap.

In some experiments, we ramp the quadrupole field \mathbf{B}_q while keeping the solenoid field \mathbf{B}_s constant. Given that the filling stage ends at time t_L , the ramping factor for the quadrupole field is $R(t - t_L)$, the magnitude of the \mathbf{B} -field varies as

$$|\mathbf{B}(t - t_L)| = |\mathbf{B}_s + R(t - t_L)\mathbf{B}_{q,max}|, \quad (4)$$

where $\mathbf{B}_{q,max}$ is the maximum value of the quadrupole field. For ramping cases, we develop a tensor-spline method to model the gradient of $|\mathbf{B}(t - t_L)|$ based on tensor-spline models for each component of \mathbf{B}_s and $\mathbf{B}_{q,max}$.

2.2. Wall loss model

When an above threshold UCN collides with the cylindrical wall or endcap boundaries, we assign it a loss probability p_{loss} according to a model based on assumed material properties [11,12,13]. After k collisions, the empirical survival probability of the UCN is

$$p_{\text{surv}}(k) = \prod_{i=1}^k [1 - p_{\text{loss}}(i)]. \quad (5)$$

We track each above threshold UCN until its empirical survival probability drops below 10^{-9} . Due to chaotic scattering effects, the symplectic integration prediction for a trajectory of an UCN does not converge in general as the time step parameter in the integration code is reduced [19]. Here, we assume that the mean survival probability at any time t for an ensemble of UCNs does not depend on the time step parameter even though the predicted survival probability of a particular UCN may depend on the time step

parameter. Although we are unaware of any proof that this assumption is true, it seems reasonable. For more discussion of this point, see [19].

We model the interaction of the neutron with the materials on the trap boundaries with a one-dimensional optical model based on Schrodinger's equation. In this approach, we assume that each neutron energy is sufficiently low so that its wavelength is very large compared to the spacing between nuclei in the wall materials. Hence, coherent effects are significant and interactions are well predicted by an optical model where the neutron potential is $V - iW$. For the cylindrical walls, we model the the neutron potential as due to layers of different homogenous materials following [11]. The materials at the endcaps at $z = -60$ cm and $z = 37.5$ cm are Teflon FEP¹ and acrylic respectively. Given that a UCN with velocity \mathbf{v} crosses the trap boundary at location \mathbf{x} and that the surface normal for the trap boundary at \mathbf{x} is $\hat{\mathbf{n}}$, we define $E_{\perp} = \frac{1}{2}m_n|\mathbf{v} \cdot \hat{\mathbf{n}}|^2$. For the endcaps, we model the probability of diffuse reflection off the wall based on Eq. 2.71 of [11] as

$$p_{\text{scat}} = \frac{E_{\perp} - \sqrt{E_{\perp}(2\alpha - 2(V_* - E_{\perp}))} + \alpha}{E_{\perp} + \sqrt{E_{\perp}(2\alpha - 2(V_* - E_{\perp}))} + \alpha}, \quad (6)$$

where

$$\alpha = \sqrt{(V_* - E_{\perp})^2 + W^2},$$

and $V_* = V - V_{He}$ where $V_{He} = 15.98$ neV. For the Teflon material, $V = 27.8$ neV and $W = 1.39\text{e-}04$ neV. For the acrylic material, $V = 121.04$ neV and $W = 4.74\text{e-}05$ neV.

The material that coats the cylindrical walls of the trap is modeled as multilayer of tetraphenyl butadiene (TPB) ($\text{C}_{28}\text{H}_{22}$), Gore-Tex (C_2F_4), graphite (C), and boron nitride (BN). The TPB used in the experiment is not deuterated and therefore contains a substantial amount of hydrogen, which has a very large incoherent scattering cross section. Since the optical model does not account for incoherent scattering, we add an additional term to account for it. The real and imaginary components of the augmented potential for

¹ Certain materials are identified in this paper to foster understanding. Such identification does not imply recommendation or endorsement by the National Institute of Standards and Technology, nor does it imply that the materials identified are necessarily the best available for the purpose.

each multilayer are

$$V = \frac{2\pi\hbar^2}{m_n} \sum_i N_i a_i,$$

and

$$W = \frac{\hbar v}{2} \sum_i N_i (\sigma_{\text{abs}}^i + \sigma_{\text{loss}}^i),$$

where for the i th nuclear isotope, N_i is nucleus density; a_i is the coherent scattering length; σ_{abs}^i is the absorption cross section; and σ_{loss}^i accounts for incoherent scattering losses. Since approximately half of the neutrons that undergo incoherent scattering will be scattered back into the ^4He and the rest will be lost, σ_{loss} is set to half of the estimated total incoherent cross section. After this modification, we solve the appropriate differential equation and determine the loss probability of the neutron as a function of E_{\perp} (Figure 2). Our model does not include the possibility of surface contamination [23] as we do not currently have a way of characterizing surface contamination quantitatively. However, for the most part, such contamination would lead to an additional marginally-trapped neutron loss mechanism. We expect that such an additional loss mechanism would reduce the systematic effect associated with marginally trapped neutrons.

After each wall collision, we scatter the neutron back into the trapping volume. Since the surface of the walls that scatter neutrons is rough, we model the reflection of the neutron with a Lambertian model [24] rather than a specular model that is appropriate for a perfectly smooth surface. In optical applications of the Lambertian model, the intensity of a reflected signal is proportional to $\cos(\theta)$ where θ is the inclination angle between the surface normal of the emitter and the direction of the reflected radiation. Hence, in our simulation studies, it follows that the cumulative distribution function (CDF) for the inclination angle between the surface normal of the wall and the direction of reflected neutron θ is

$$F_L(\theta) = \frac{1 - \cos(2\theta)}{2},$$

where $0 \leq \theta \leq \frac{\pi}{2}$. The azimuthal angle ϕ is a uniformly distributed random variable between 0 and 2π . In contrast, for a diffuse reflection model based on a uniform intensity model, the CDF of the direction cosine of the reflected neutron is

$$F_U(\cos(\theta)) = \cos(\theta),$$

where $0 \leq \cos(\theta) \leq 1$. Later, in Section 4.3, we quantify the variation of the estimated lifetime of trapped neutrons for different neutron reflectivity models.

3. Survival Analysis Model

3.1. Mathematical preliminaries

In survival analysis, for any loss mechanism, the loss time T of an object (in our case a neutron) created at time $t = 0$ is a random variable with survival probability $S(t)$ where

$$S(t) = \Pr(T > t).$$

For a continuous $S(t)$, one can define the hazard function $\lambda(t)$ which is the instantaneous loss rate at time t given that the object of interest survives until time t as follows.

$$\lambda(t) = \lim_{\Delta t \rightarrow 0} \frac{\Pr(t \leq T \leq t + \Delta t | T \geq t)}{\Delta t},$$

where $\Pr(t \leq T \leq t + \Delta t | T \geq t)$ is the conditional probability that the loss time T falls in the interval $[t, t + \Delta t]$ given that T is no less than t . Based on the well known conditional probability equality $\Pr(A|B) = \Pr(A \cap B) / \Pr(B)$, one gets the following well known expression for the hazard function

$$\lambda(t) = \frac{1}{S(t)} \lim_{\Delta t \rightarrow 0} \frac{S(t) - S(t + \Delta t)}{\Delta t} = -\frac{d \log S(t)}{dt}.$$

For the neutron β -decay loss mechanism, the associated hazard function is $\lambda_\beta = \frac{1}{\tau_n}$ where τ_n is the neutron lifetime. For the mechanism associated with wall losses of marginally trapped UCNs, we expect $\lambda(t)$ to vary with time since high energy UCNs should, on average, be lost at a higher rate compared to low energy UCNs. In general, for any loss mechanism,

$$S(t) = \exp(-\Lambda(t)),$$

where the cumulative hazard function $\Lambda(t)$ is

$$\Lambda(t) = \int_{t=0}^t \lambda(t) dt.$$

Thus, the survival probability function associated with β -decay is $S_\beta(t) = \exp(-\lambda_\beta \tau_n) = \exp(-\frac{t}{\tau_n})$.

In a competing risks model, the multivariate survival probability function is $S(t_1, t_2, \dots, t_K)$ where

$$S(t_1, t_2, \dots, t_K) = \Pr(T_1 \geq t_1, T_2 \geq t_2, \dots, T_K \geq t_K).$$

The term T_i is a random variable representing the loss time associated with the i th loss mechanism. In general, for $i \neq j$, the random variables T_i and T_j need not be independent. The actual loss time of the object of interest is $T = \min(T_1, T_2, \dots, T_K)$ where K is the number of loss mechanisms. One can recover the survival probability function for the j th loss mechanism at time t by evaluating the multivariate one at $t_j = t$ and $t_i = 0$ for all other $i \neq j$. The cause-specific hazard function for the j th loss mechanism is λ_j where

$$\lambda_j(t) = -\frac{\partial \log S}{\partial t_j} \Big|_{t_1=t_2=\dots, t_K=t}. \quad (7)$$

For the NIST experiment, we assume that all neutron loss mechanisms are independent. Given this independence assumption, we can write $S(t_1, t_2, \dots, t_K) = \prod_{j=1}^K S_j(t_j)$ where $S_j(t)$ is the survival probability function associated with the j th loss mechanism. Further, for each independent loss mechanism, the cause-specific loss mechanism for the j th loss mechanism is

$$\lambda_j(t) = -\frac{d \log S_j(t)}{dt}. \quad (8)$$

For our problem, the joint hazard and survival probability functions of an UCN due to all loss mechanisms at time t are $\sum_{j=1}^K \lambda_j(t)$ and $\exp(-\sum_{j=1}^K \Lambda_j(t))$ respectively.

3.2. Conditional survival probability

If an UCN is created at time $t = 0$, the conditional survival probability associated with the first loss mechanism given the the UCN survives all loss mechanisms until at least time t_L is

$$S(t, t_L, t_L, \dots, t_L) / S(t_L, t_L, t_L, \dots, t_L),$$

for $t \geq t_L$. In the NIST experiment, we model the creation time of any UCN during the filling stage as a uniform random variable between $t = 0$ and

$t = t_L$ where t_L is the time spent filling (loading) the trap. For the first loss mechanism, the conditional survival probability for an UCN that survives the filling stage is

$$S_1(t|T \geq t_L) = \left[\int_{s=0}^{s=t_L} S(t-s, t_L-s, \dots, t_L-s) ds \right] / \left[\int_{s=0}^{s=t_L} S(t_L-s, t_L-s, \dots, t_L-s) ds \right] \quad (9)$$

A similar statement applies to the other loss mechanisms. Aside from β -decay and wall losses, neutrons can be lost by absorption processes associated with impurities (primarily ^3He capture) and by upscattering. We expect the hazard function associated with upscattering to vary with temperature. However, for the ideal case where temperature is constant, the hazard function for upscattering is a constant $\lambda_u = \frac{1}{\tau_u}$. From first principle arguments, the hazard function associated with an energy-independent absorption process is a constant $\lambda_a = \frac{1}{\tau_a}$. We define λ_* to be sum of the three hazard functions associated with β -decay, upscattering and an additional energy-independent absorption process. Each of these three hazard functions is a constant in our model. Thus,

$$\lambda_* = \frac{1}{\tau_*} = \frac{1}{\tau_n} + \frac{1}{\tau_u} + \frac{1}{\tau_a}. \quad (10)$$

We stress that λ_* does not account for the hazard function associated with the wall loss mechanism. Next, we develop a model that enables us to directly estimate λ_* from experimental data given that we have an estimate for the survival probability function $S_M(t)$ associated with the wall loss mechanism.

Following arguments in [18], given the production rate of below and above threshold UCNs during the filling stage are r_- and r_+ , we predict the expected number of below threshold UCNs at the end of filling stage (t_L) as

$$\langle N_-(t_L) \rangle = r_- \int_{s=0}^{t_L} \exp(\lambda_*(s - t_L)) ds. \quad (11)$$

The predicted number of above threshold UCNs at the end of the filling stage is

$$\langle N_+(t_L) \rangle = r_+ \int_{s=0}^{t_L} S_M(t_L - s) \exp(\lambda_*(s - t_L)) ds, \quad (12)$$

where $S_M(t)$ is survival probability function associated with wall losses of above threshold UCNs. As stated earlier, $S_M(t)$ has a non-exponential form in general.

Given that an above threshold UCN survives the filling stage, the conditional survival probability associated with wall losses is

$$S_M^+(t) = S_M(t|T \geq t_L) = \left[\int_{s=0}^{t_L} S_M(t - s) \exp(\lambda_*(s - t_L)) ds \right] / \left[\int_{s=0}^{t_L} S_M(t_L - s) \exp(\lambda_*(s - t_L)) ds \right]. \quad (13)$$

For loss mechanisms with exponential survival probability functions, $S(t|T > t_L) = S(t - t_L)$. Hence, for times $t > t_L$,

$$\langle N(t) \rangle = \langle N_-(t_L) \rangle \left[1 + \frac{\langle N_+(t_L) \rangle}{\langle N_-(t_L) \rangle} S_M^+(t) \right] \exp(-\lambda_*(t - t_L)). \quad (14)$$

We can rewrite the above as

$$\langle N(t) \rangle = \langle N_-(t_L) \rangle [1 + \Delta(t)] \exp(-\lambda_*(t - t_L)), \quad (15)$$

where the time-dependent “distortion” term Δ is

$$\Delta(t) = \frac{\langle N_+(t_L) \rangle}{\langle N_-(t_L) \rangle} S_M^+(t). \quad (16)$$

Based on the above, the expected loss rate of neutrons lost due to β -decay, absorption, and upscattering are $r_\beta(t) = \frac{\langle N(t) \rangle}{\tau_n}$, $r_a(t) = \frac{\langle N(t) \rangle}{\tau_a}$, and $r_u(t) = \frac{\langle N(t) \rangle}{\tau_u}$ respectively. Given that upscattering losses are unobservable and absorption events yield events that are indistinguishable from β -decay events, the overall predicted detection rate is

$$r_{det}(t) = \langle N(t) \rangle \left[\frac{p_\beta}{\tau_n} + \frac{p_a}{\tau_a} \right] \quad (17)$$

where p_β and p_a are detection probabilities for two loss mechanisms.

3.3. Contamination ratio

Following [18], we can decompose $\langle N(t) \rangle$ into exponential and non-exponential components as follows.

$$\langle N(t) \rangle = f_{exp}(t) + f_c(t), \quad (18)$$

where

$$f_{exp}(t) = \langle N_-(t_L) \rangle [1 + \Delta(t_{end})] \exp(-\lambda_*(t - t_L)), \quad (19)$$

and

$$f_c(t) = \langle N_-(t_L) \rangle [\Delta(t) - \Delta(t_{end})] \exp(-\lambda_*(t - t_L)). \quad (20)$$

The ratio of the non-exponential and exponential terms can be regarded as a contamination ratio r_c where

$$r_c(t) = \frac{\Delta(t) - \Delta(t_{end})}{1 + \Delta(t_{end})}. \quad (21)$$

We emphasize that $\Delta(t)$ and $f_c(t)$ are nonlinear functions of λ_* . In Section 4, we estimate λ_* directly from experimental data given a Monte Carlo estimate of $S_M(t)$ based on a physical model for the wall loss probability and how surviving neutrons are reflected back into the trapping volume. The uncertainty of λ_* depends, in part, on imperfect knowledge of: the wall loss probability model; how surviving neutron reflect off the walls; the spatially varying fluence of the thermal beam that produces UCN in the trap; and the usual counting statistics variability in the observed data.

4. Experimental Application

4.1. Prediction model

For experimental data corresponding to a particular subset of runs from the NIST experiment, we estimate λ_* by fitting a model to experimental data based on Eqns. 15 and 17. The primary (background plus neutron events) data are acquired for a static trapping potential. Background measurements are also acquired in non-trapping runs and subtracted from the primary observations [5]. Our primary goal is to understand systematic measurement errors and associated uncertainties associated with marginally trapped neutrons and other loss mechanisms. Hence, we analyze data corresponding to an experiment where we did not ramp the magnetic field in order to maximize the systematic effects of marginally trapped neutrons.

More specifically, for bins that are 1 s wide, we predict the number of background-corrected counts in the k th bin as

$$\hat{n}_k = A\lambda_*\delta_t[1 + \Delta(t_k)]\exp(-\lambda_*(t_k - t_L)) + r_{bg}\delta_t, \quad (22)$$

where $\delta_t = 1$ s is the resolution at which we determine survival probabilities by our Monte Carlo method, t_k is the midpoint of the k th time bin, and A , r_{bg} and λ_* are adjustable model parameters determined by our modeling fitting procedure. Since the width of the bins for the observed data is 15 s, we aggregate predictions at the 1 s scale to get predictions at the 15 s scale of interest.

Given that we estimate these parameters to be \hat{A} and $\hat{\lambda}$, we can predict the expected number of below threshold trapped UCNs at $t = t_L$ as

$$\langle \widehat{N_-(t_L)} \rangle = \frac{\hat{A}\hat{\lambda}_{tot}}{p_\beta(\hat{\lambda}_{tot} - \lambda_a - \lambda_u) + p_a\lambda_a}, \quad (23)$$

where the hazard functions λ_a and λ_u and detection probabilities p_a and p_β are determined from other experiments and/or theoretical arguments.

4.2. Estimation details

In the NIST experiment, the cold neutron beam that produces the UCNs is collimated. Based on an uncollimated measured beam profile and knowledge of the geometry of the collimator, we estimate a spatially varying neutron fluence image at the entrance to the detector (Figure 3) and an associated probability density function for the intersection of any neutron trajectory and the plane at $z = -60$ cm. Based on this probability density function, we simulate intersection points with the Von Neuman rejection sampling method [25,26]. For each intersection point, we simulate a neutron velocity direction vector \hat{v} that has length 1. For the case where there is no beam divergence, \hat{v} is parallel to the axial direction of the trap. For the case of non-zero divergence, we simulate \hat{v} such that its direction cosine with respect to the z -direction is uniformly distributed in the interval $(\cos(\theta_{\max}), 1)$. That is, simulated realization of \hat{v} fall within a cone. The location of the UCN produced by a neutron is $(x_o, y_o, z_o) + L_{sim}\hat{v}$ where (x_o, y_o, z_o) is the simulated location of the neutron at $z_o = -60$ cm, and L_{sim} is the simulated distance traveled by the neutron before a UCN is produced. Given the initial location of the UCN, we simulate its initial velocity as described earlier.

Given the initial velocity and position of an UCN, we determine its trajectory with the symplectic integration method described in Section 2.1.

For the case of no beam divergence, the production rate of above threshold UCNs, r_+ (Eq. 12), produced in the trap at random times in the interval $(0, t_L)$ is 4.2 times larger than the production rate, r_- (Eq. 11), of below threshold UCNs for the nominal trapping volume defined by $-37.5 \text{ cm} \leq 37.5 \text{ cm}$ (Figure 4). The energy range of simulated above threshold UCNs is 139 neV to 246 neV. In general, the UCN wall collision rate increases with energy (Figure 5). Based on Monte Carlo estimates of $S_M(t)$ at discrete times $(0, 1, 2, \dots, 5500) \text{ s}$, we determine $\Delta(t)$ (Eq. 16) on a discrete time grid (Figure 6). Recall, the theoretical value of $\Delta(t_L)$ equals $\frac{\langle N_+(t_L) \rangle}{\langle N_-(t_L) \rangle}$. Even though the relative production of above and below threshold UCNs is 4.2, $\frac{\langle N_+(t_L) \rangle}{\langle N_-(t_L) \rangle}$ is approximately 0.41. That is, a large fraction of above threshold UCN is lost during the filling stage. Since UCNs with energy greater than 246 neV would be lost to the walls in approximately a few seconds or less, such high energy UCNs would have a negligible effect on $\Delta(t)$ for $t - t_L > 10 \text{ s}$. Thus, extending the maximum energy of simulated above threshold UCN would have a negligible effect on our estimate of λ_* .

We average 40 independent estimates of $S_M(t)$ from independent Monte Carlo experiments to get an overall estimate of $S_M(t)$ and $\Delta(t)$. Given a wall loss probability model that accounts for incoherent scattering, we determine the mean lifetime of the neutron in the trap to be 700 s with a standard uncertainty of 57 s (Table 1, Figure 7). In this standard approach, the model is assumed to be valid and deviations between observations and predicted values based on perfect knowledge of the model parameters are due to counting statistics. To quantify the component of uncertainty due to imperfect knowledge of $S_M(t)$ due to sampling variability, we simulated bootstrap [27] replications of our estimate of $S_M(t)$ by resampling with replacement the 40 independent estimates of $S_M(t)$ that we averaged in the first study. For each bootstrap replication of the average $S_M(t)$, we refit our model to the same observed data. The bootstrap estimate of uncertainty due to sampling variability of $S_M(t)$ is 2.4 s.

4.3. Systematic effects

For comparison, when we set $\Delta(t) = 0$, i.e., when we neglect wall losses, we estimate the lifetime to be 655 s with an estimated uncertainty of 51 s (Table 1). When we estimate $S_M(t)$ based on a wall loss model that neglects incoherent scattering effect for the cylindrical boundary, we estimate the

neutron lifetime to be 708 s with an associated 1-sigma uncertainty of 59 s. Based on this, we estimate the component of uncertainty contributed by imperfect knowledge of the wall loss probability model to be 8 s.

For the primary wall loss model that accounts for incoherent scattering, we estimate λ_* for different definitions of the trapping volume. In particular, we vary the lower axial boundary of the trapping volume, z_{min} , from -37.5 cm to -35 cm and -40 cm (Table 2). We fit a linear model to predict the expected value of $\hat{\lambda}$ as a function of z_{min} . The estimated slope of this linear model and its associated uncertainty are -0.55 s/cm and 0.40 s/cm.

In a similar study, we vary the time-step parameter in the symplectic integration algorithm (Table 2). The estimated slope of a linear model to predict the lifetime as a function of the time step is 2.9×10^{-4} where the uncertainty is 3.79×10^{-4} . Based on this result, the expected difference in a lifetime estimate based on a simulation where the time step parameter $dt = 5.0 \times 10^{-5}$ and where $dt = \epsilon$ where ϵ is arbitrarily close to 0 s, is 1.4 (1.9) s.

Variation in the beam divergence parameter θ_{max} produces a statistically significant variation in the lifetime estimate (Figure 8) because the distribution of the initial potential energy of an UCN created in the trap depends on θ_{max} . Thus, even though the distribution of the initial kinetic energy of an UCN produced in the trap does not depend on θ_{max} , the distribution of the initial total energy of the UCN depends on θ_{max} . We estimate θ_{max} to be 3.0 degrees by matching the expected value of θ in the simulation to that predicted based on analysis of the dispersion of scattering plane orientations in mosaic crystals relative to their mean value [28]. In [28], the angle between the random orientation of a particular scattering plane and the mean orientation is a truncated Gaussian. Since the slope of the fitted line in Figure 8 is $-0.97(0.16)$ s deg $^{-1}$, we estimate the systematic error due to ignoring beam divergence effects to be approximately 2.9 s. As a caveat, to estimate an uncertainty, we assume a one-to-one relationship between the standard deviation of the random mosaic crystal orientations and the standard deviation of direction cosines in our simulation study. Further, in our beam divergence study, the probability distribution function for the direction cosine of a UCN at $z = -60$ cm is a uniform distribution. In contrast, for the mosaic crystal model, the angle between the mean orientation and any random orientation is a truncated Gaussian distribution.

Our estimate of λ_* systematically depends on the assumed model for how surviving neutrons are reflected back into the trapping volume (Table 3). Because of surface roughness effects, the two diffuse models are much more

Table 1. Model parameter estimates for NIST experimental data for a static potential. Survival probability function associated with wall loss determined for two scenarios; incoherent scattering in neutrons in materials is either neglected or accounted for. Beam divergence neglected. The time step parameter for all cases is $dt = 5.0\text{e-}05$ s.

case	account for incoherent scattering	account for marginally trapped neutrons	A	τ_* (s)	r_{bg} (s^{-1})	χ^2/df	p-value
a	yes	yes	57943 (3883)	700 (57)	1.8 (1.8)	1.080	0.2234
b	yes	no	76114 (4531)	655 (51)	2.3 (1.7)	1.085	0.2118
c	no	yes	41558 (2856)	708 (59)	1.8 (1.8)	1.082	0.2187

plausible than the specular model. Hence, the difference between the estimates for the diffuse models (1.3 s with an uncertainty of 1.5 s) is relevant for estimation of a systematic uncertainty due to imperfect knowledge of the model for neutron reflection.

In all earlier studies in this work, we account for gravity and spatial variation in the cold beam fluence. Failure to account for gravity shifts the estimate of τ_* downward by 5.1 s (standard uncertainty is 1.6 s) (Table 4). We expect this shift for two reasons. First, gravity changes the distribution of the initial potential energy of UCNs and hence the distribution of the initial energy of UCNs. Second, for the cases studied here, gravity reduces the minimum potential energy on the nominal trapping volume boundary from 139 neV to 135.5 neV. Recall, this minimum potential energy is the threshold for defining a marginally trapped UCN.

Failure to account for spatial variation in assumed neutron beam fluence shifts the estimate of τ_* upward by 7.5 s (standard uncertainty is 1.6 s) (Table 4). As a summary, we list estimates of systematic uncertainties associated with the effects studied here in Table 5.

For the NIST experiment, we expect the walls of the trap to vibrate and perturb the energy of UCNs that survive wall collisions and are reflected back into the trapping volume. For more discussion of this effect for a simplified 1-D vibrational model for a magneto-gravitational trap, see Salvat and Walstrom [29]. Since the wall loss probability of an UCN depends on its E_\perp

Table 2. For a static potential experiment, dependence of estimated τ_* on lower axial boundary of nominal trapping volume (z_{min}) and time-step dt in symplectic integration algorithm. We account for wall losses when estimating τ_* . Beam divergence effects neglected. Reported uncertainties account for uncertainty of $\Delta(t)$ (Eq. 16) due to Monte Carlo sampling variability.

dt (s)	z_{min} (cm)	$\tau_*(s)$
1.0e-04	-40	703.3(1.5)
1.0e-04	-35	700.5(1.5)
1.0e-04	-37.5	701.9(1.1)
5.0e-05	-37.5	699.9(2.4)
2.5e-05	-37.5	699.9(2.8)

Table 3. For a static potential experiment, dependence of estimated τ_* on neutron scattering modeling. Beam divergence neglected. Reported uncertainties account for uncertainty of $\Delta(t)$ (Eq. 16) due to Monte Carlo sampling variability.

reflection model	dt (s)	z_{min} (cm)	$\tau_*(s)$
diffuse Lambertian	1.0e-04	-37.5	701.9(1.1)
diffuse uniform	1.0e-04	-37.5	703.2(1.0)
specular	1.0e-04	-37.5	713.5(1.5)

Table 4. For a static potential experiment, dependence of estimated τ_* on gravity and spatial variation of neutron beam (Figure 2). For all cases, the wall loss probability model accounts for incoherent scattering. We assume a diffuse Lambertial model for neutron reflections. No beam divergence. The time step parameter is $dt = 1.0e-04$. The uncertainties account for imprecise knowledge of the $\Delta(t)$ (Eq. 16) due to Monte Carlo sampling variability.

gravity accounted for	beam profile accounted for	$\tau_*(s)$
yes	yes	701.9(1.1)
no	yes	694.4(1.2)
yes	no	707.0(1.2)

Table 5. For a static potential experiment, systematic effects and associated uncertainties for τ_* measurement due to wall losses of marginally trapped UCNs. Effects that are not statistically significant are indicated with asterisks.

effect	correction	uncertainty
wall loss model	none	8 s
neutron reflections model	none	1.3 s
beam divergence	-2.9	2.9 s
beam profile model	none	NA
upscattering	none	$\ll 1$ s
^3He absorption	NA	NA
mechanical vibrations	none	NA
time step	none	1.9 s *
choice of z_{min}	none	1 s *
Total	-2.9 s	8.9 s

value, energy perturbations would affect the survival probability of above threshold UCNs for a static trap experiment. Energy perturbations due to mechanical vibrations would also affect how well above threshold UCNs are purged (and how well below threshold UCNs are retained) when magnetic fields are ramped. Development of a realistic three-dimensional model for the effect of mechanical vibrations for the NIST experiment is an important and very challenging research topic beyond the scope of this study.

5. Ramping Studies

In magnetic trapping experiments, one can purge above threshold UCNs from the trap by ramping the trapping potential down and then ramping it back up to its original value [4,30]. In a background-free simulation experiment, we reduced the quadrupole field from its maximum value to an adjustable fraction of its initial value (Figure 9). We denote this fraction as a ramping fraction. For any given ramping schedule, we determined the conditional survival probability for all UCNs (rather than just above threshold UCNs) that survive ramping by a direct simulation method for a fixed value of $\tau_* = 686$ s. Based on this conditional survival probability, we simulate high-count β -decay data under the assumption that the observation rate in narrow 1 s width bins is well approximated as $\langle N(t) \rangle / \tau_n$. We fit the Eq. 22 prediction model to simulated data with $\Delta(t) = 0$. That is, we ignore wall losses. For ramping fractions less than approximately 0.3, the systematic error of the estimated lifetime is very small (Figure 10).

The benefits of purging above threshold UCNs by field ramping come with a cost. That is, we also purge a non-negligible fraction of initially below threshold UCNs. For instance, for the case where the ramping fraction is 0.3, the fraction of surviving above threshold UCNs immediately after ramping ends is 0.00072. However, the fraction of originally below threshold UCNs is reduced to 0.30(0.02).

There are other field ramping strategies to purge above threshold UCNs than the one considered here. For instance, one could fill the trap with the trapping potential reduced to its minimal value and then ramp it after the filling stage ends. In a simulation experiment, we compared this alternative ramping strategy to ours. We simulated UCNs with the same initial locations and initial velocities and tracked them for both strategies. In order to purge all but 0.0072 of the above threshold UCNs, the fraction of below threshold UCNs retained by the alternative upramping scheme is 0.06(0.01). Thus,

for this case, the relative number of below threshold UCNs after ramping is less for the alternative ramping strategy compared to the ramping strategy implemented in our simulation study. To help explain the result, we note that in the alternative ramping schedule, the quadrupole field is maintained at a much lower initial value than in the original ramping schedule. Hence, during the filling stage, the energy threshold that defines a marginally trapped UCN is lower for the alternative ramping scheme compared to the original scheme.

6. Summary

We developed a competing risks survival analysis model to account for losses due to the joint effect of β -decay losses, wall losses of marginal trapped neutrons, and an unspecified absorption mechanism. We determined the survival probability function associated with the wall loss mechanism by a Monte Carlo method based on physical models for the loss probability of above threshold UCNs that interact with materials in cylindrical wall and endcaps of the trap. In our approach, we track above threshold UCNs in the trap with a computer intensive symplectic integration method. For any trapping volume, we objectively define above threshold UCNs as those with total energy greater than the minimum potential energy on the trap boundary. Hence, there is no need to track UCNs below this threshold.

Based on estimated survival probabilities, we constructed a prediction model for observed data acquired in a magnetic trapping neutron lifetime experiment at NIST where the trapping potential is static. Based on a fit of this model to a subset of the NIST experimental data, we determined the mean lifetime of neutrons in the trap to be 700 s with an uncertainty of approximately 60 s – considerably less than the current best estimate of (880.1 ± 1.1) s. The source of this discrepancy is an ongoing research topic; experiments are underway to determine if this discrepancy can be explained by neutron capture by ^3He impurities in the trapping volume. In our model, the largest source of systematic uncertainty is associated with imperfect knowledge of the wall loss probability model (8 s) (Table 5). If we neglect the effect of marginally trapped neutrons, for the static case considered here, the estimated lifetime of the neutron is shifted downward by 45 s (Tables 1).

In a Monte Carlo experiment, we demonstrated that when the trapping potential is ramped down and then back again, systematic error due to wall losses of marginally trapped UCNs can be suppressed to a very low level. For a particular case, Monte Carlo simulation studies showed that this ramping

strategy is more efficient than one where neutrons are trapped when the field is fully ramped and then increased to its maximum value. From a practical perspective, our stochastic model and associated Monte Carlo methods should be helpful to guide design of field ramping strategies to purge above threshold UCNs in magnetic trapping and related trapping experiments.

Acknowledgements. We thank Grace Yang for useful comments. We acknowledge the support of the NIST, US Department of Commerce, in providing support, including the neutron facilities used in this work. This work is also supported in part by the US National Science Foundation under Grant No. PHY-0855593 and the US Department of Energy under Grant No. DE-FG02-97ER41042. Contributions by staff of NIST, an agency of the US government, are not subject to copyright in the US.

References

- [1] J. Beringer et al. (Particle Data Group), PR D86, 010001 (2012) (URL: <http://pdg.lbl.gov>)
- [2] F.E. Wietfeldt and G.L. Greene, Rev. of Mod. Phys. 8383 1173 (2011)
- [3] A. T. Yue, M. S. Dewey, D. M. Gilliam, G. L. Greene, A. B. Laptev, J. S. Nico, W. M. Snow, and F. E. Wietfeldt Phys. Rev. Lett. 111, 222501 (2013)
- [4] S. Paul, Nucl. Instr. and Methods A611 (2009) 157.
- [5] H. P. Mumm, M. G. Huber, A. T. Yue, A. K. Thompson, M. S. Dewey, C. R. Huffer, P. R. Huffman, K. W. Schelhammer, C. OShaughnessy and K. J. Coakley, Measuring the Neutron Lifetime with Magnetically Trapped Ultracold Neutrons, 2012 Next Generation Experiments to Measure the Neutron Lifetime Workshop, World Scientific, pp. 121-134, 2014
- [6] P. R. Huffman, C. R. Brome, J. S. Butterworth, K. J. Coakley, M. S. Dewey, S. N. Dzhosyuk, R. Golub, G. L. Greene, K. Habicht, S. K. Lamoreaux, C. E. H. Mattoni, D. N. McKinsey, F. E. Wietfeldt, J. M. Doyle Nature 403, 62-64 (6 January 2000)
- [7] R. Picker, I. Altarev, J. Brcker, E. Gutsmedl, J. Hartmann, A. Mller, S. Paul, W. Schott, U. Trinks, and O. Zimmer, J. Res. Natl. Inst. Stand. Technol. 110, 357-360 (2005)
- [8] K. Leung and O Zimmer, Nucl. Instr. Methods A611 (2009) 181.
- [9] P.L. Walstrom, J.D. Bowman, S.I. Penttila, C. Morris, A. Saunders, Nucl. Instr. Methods A599 (2009) 82.

- [10] R. Golub and J.M. Pendlebury, Phys. Lett. 53A, 133 (1975).
- [11] R. Golub, D. Richardson, S.K. Lamoreaux, Ultra-Cold Neutrons, Taylor and Francis, 1991
- [12] A. Steyerl, S. S. Malik, A. M. Desai, and C. Kaufman, Phys. Rev. C 81, 055505 (2010)
- [13] C.M. Oshaughnessy, PhD thesis, North Carolina State University, 2010
- [14] M. Gail, Biometrics, 209-222. (1975).
- [15] R. L. Prentice, J. D. Kalbfleisch, A. V. Peterson, Jr., N. Flournoy, V. T. Farewell and N. E. Breslow, Biometrics, Vol. 34, No. 4 (Dec., 1978), pp. 541-554
- [16] J. D. Kalbfleisch and R. L. Prentice The Statistical Analysis of Failure Time Data, Second Edition, John Wiley & Sons, Inc. 2002
- [17] H. Putter, M. Fiocco and R. B. Geskus, Statist. Med. 2007; 26:2389-2430
- [18] K.J. Coakley, Stochastic modeling and simulation of marginally trapped neutrons, 2012 Next Generation Experiments to Measure the Neutron Lifetime Workshop, World Scientific, pp. 65-74, 2014
- [19] K. J. Coakley, J. M. Doyle, S. N. Dzhosyuk, L. Yang, P. R. Huffman, J. Res. Natl. Inst. Stand. Technol. 110, 367-376 (2005)
- [20] R. I. McLachlan and P. Atela, Nonlinearity 5, 541-562 (1992).
- [21] P.J. Channel and C. Scovel, Nonlinearity 3, 231 (1990).
- [22] C. de Boor, A practical guide to splines, Springer-Verlag, New York (1978).
- [23] E. Korobkina, R. Golub, J. Butterworth, P. Geltenbort, and S. Arzumov, Temperature dependence of ultracold neutron loss rates, Phys. Rev. B 70 (3) (2004) 035409
- [24] C. M. Goral, K. E. Torrance, D. P. Greenberg and B. Battaile, Modeling the Interaction of Light Between Diffuse Surfaces, Comput. Graphics, Volume 18, Number 3, (1984), pp. 213-222.

- [25] J. von Neumann, “Various techniques used in connection with random digits. Monte Carlo methods”, J. Res. Natl. Bur. Stand., 12 (1951), pp. 3638.
- [26] Robert, C.P. and Casella, G. “Monte Carlo Statistical Methods” (second edition). New York: Springer-Verlag, 2004.
- [27] B. Efron and R.J. Tibshirani, An Introduction to the Bootstrap, Monographs on Statistics and Applied Probability, Chapman and Hall/ CRC Press, (1993)
- [28] C.E.H. Mattoni , C.P. Adams , K.J. Alvine , J.M. Doyle , S.N. Dzhosyuk, R. Golub , E. Korobkina, , D.N. McKinsey, A.K. Thompson, , L. Yang H. Zabel P.R. Huffman, A long wavelength neutron monochromator for superthermal production of ultracold neutrons Physica B 344 (2004) 343-357
- [29] D.J. Savat and P.L. Walstrom, Vibration-induced loss of ultra-cold neutrons in a magneto-gravitational trap, 2012 Next Generation Experiments to Measure the Neutron Lifetime Workshop, World Scientific, pp. 87-96, 2014
- [30] L. Yang, PhD thesis, Harvard University, 2006.

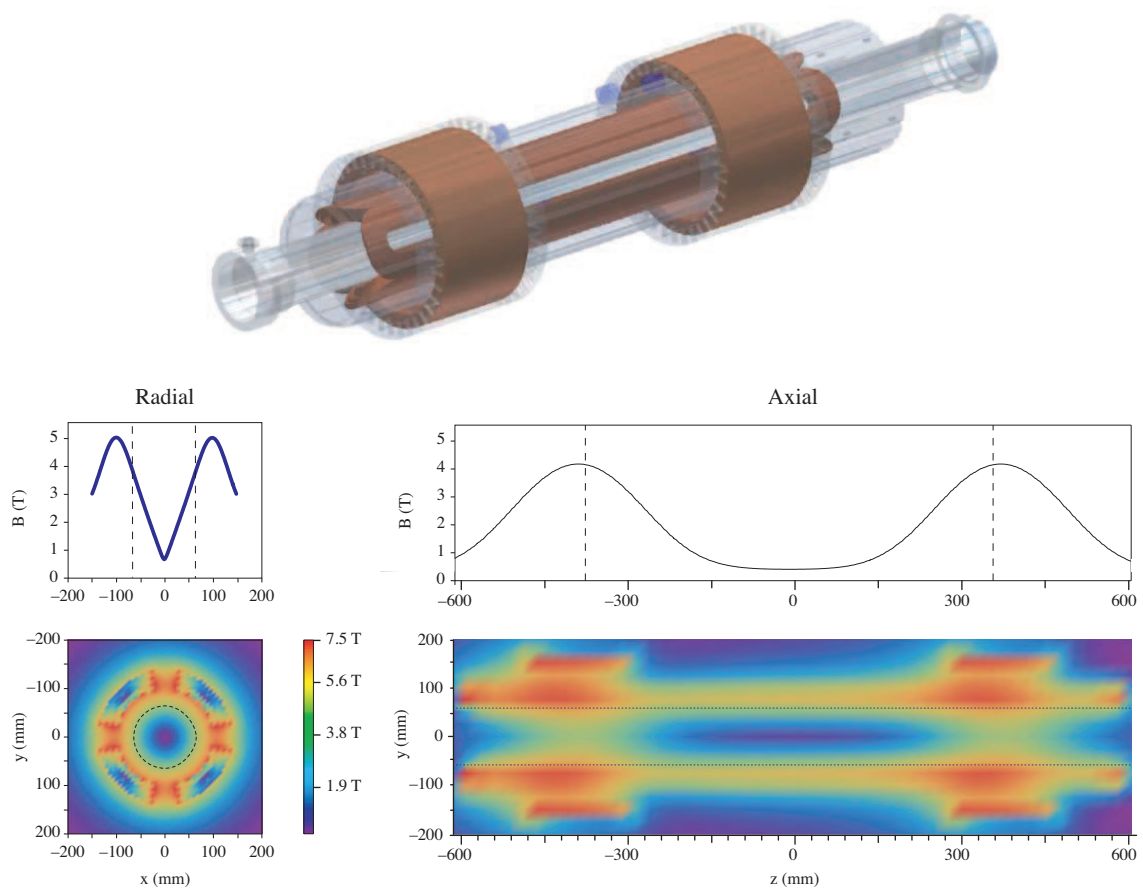


Figure 1: Magnetic field profiles in the NIST magnetic trapping experiment.

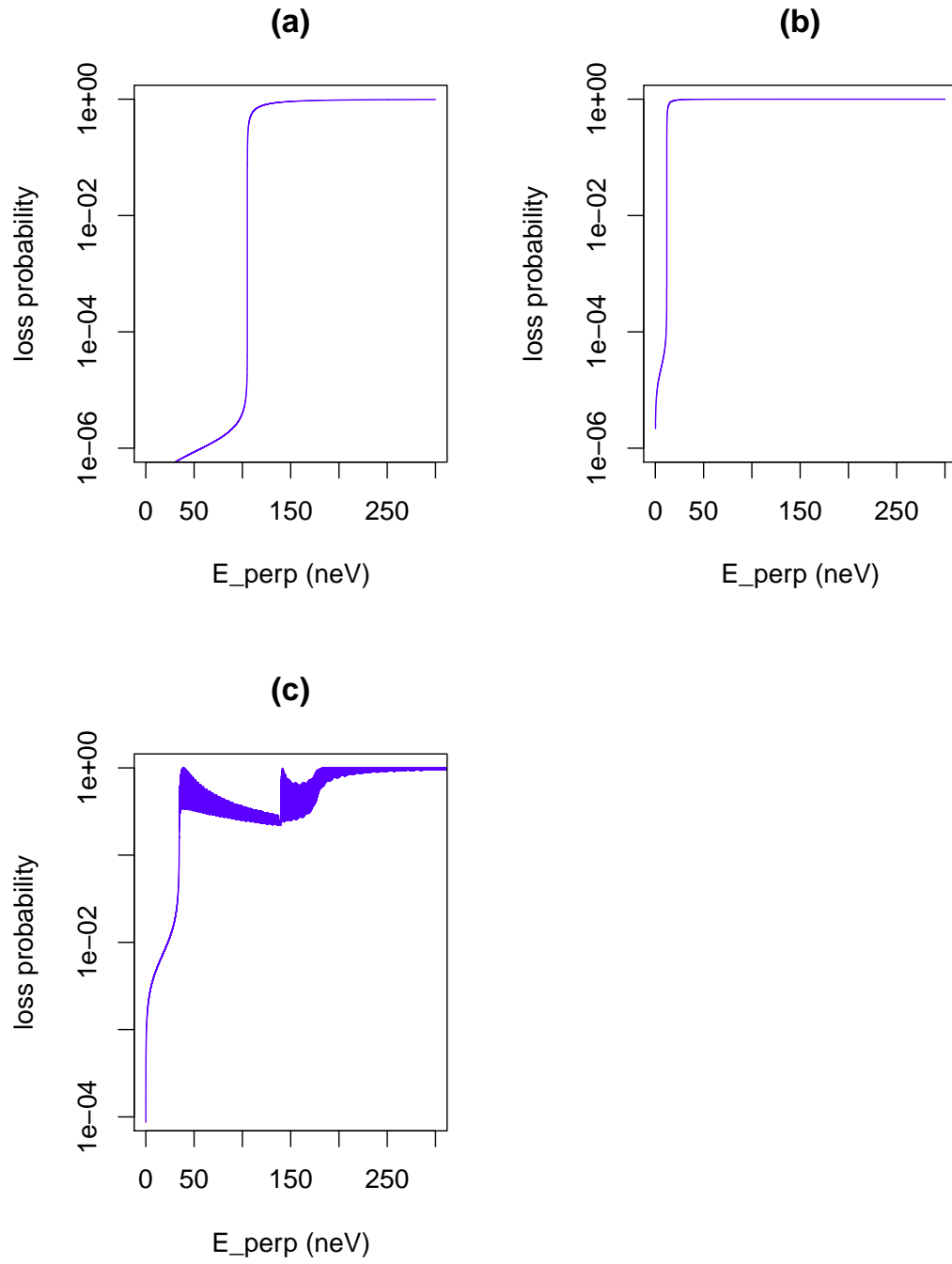


Figure 2: Loss probabilities for (a) the Teflon coated endcap; (b) the acrylic coated endcap and (c) multilayers at cylindrical wall.

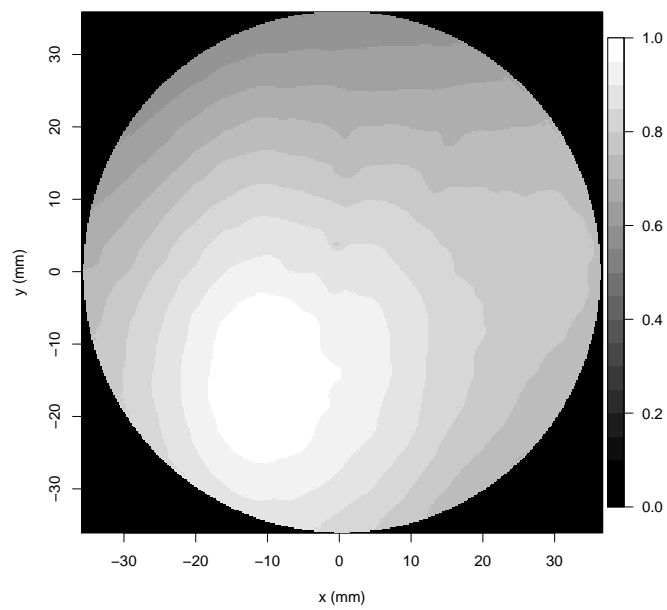


Figure 3: Model for neutron fluence in NIST magnetic trapping experiment at trap entrance.

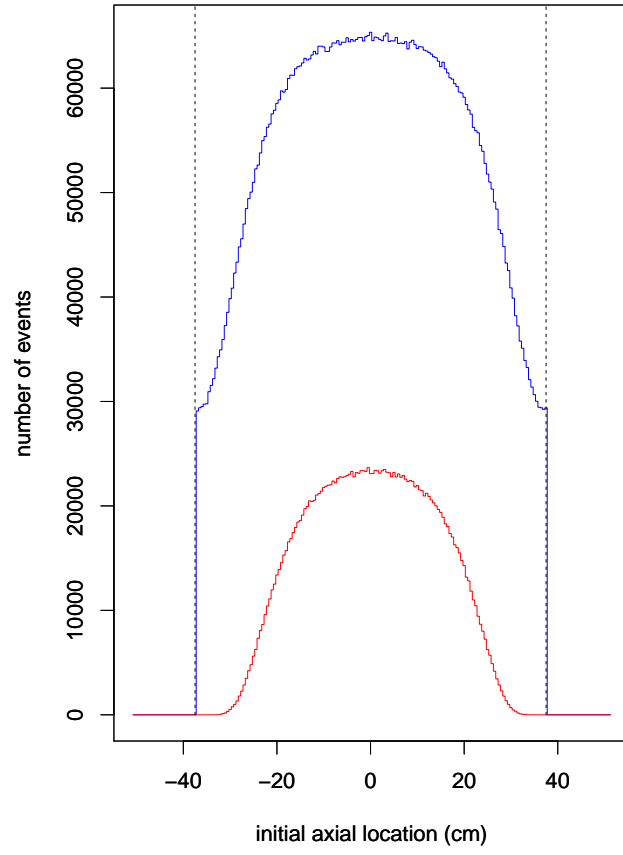


Figure 4: For a static trap where the trapping volume is defined to be $-37.5 \text{ cm} \leq z \leq 37.5 \text{ cm}$, the ratio of above threshold to below threshold UCNs is 4.22 for energies between approximately 139 neV to 246 neV.

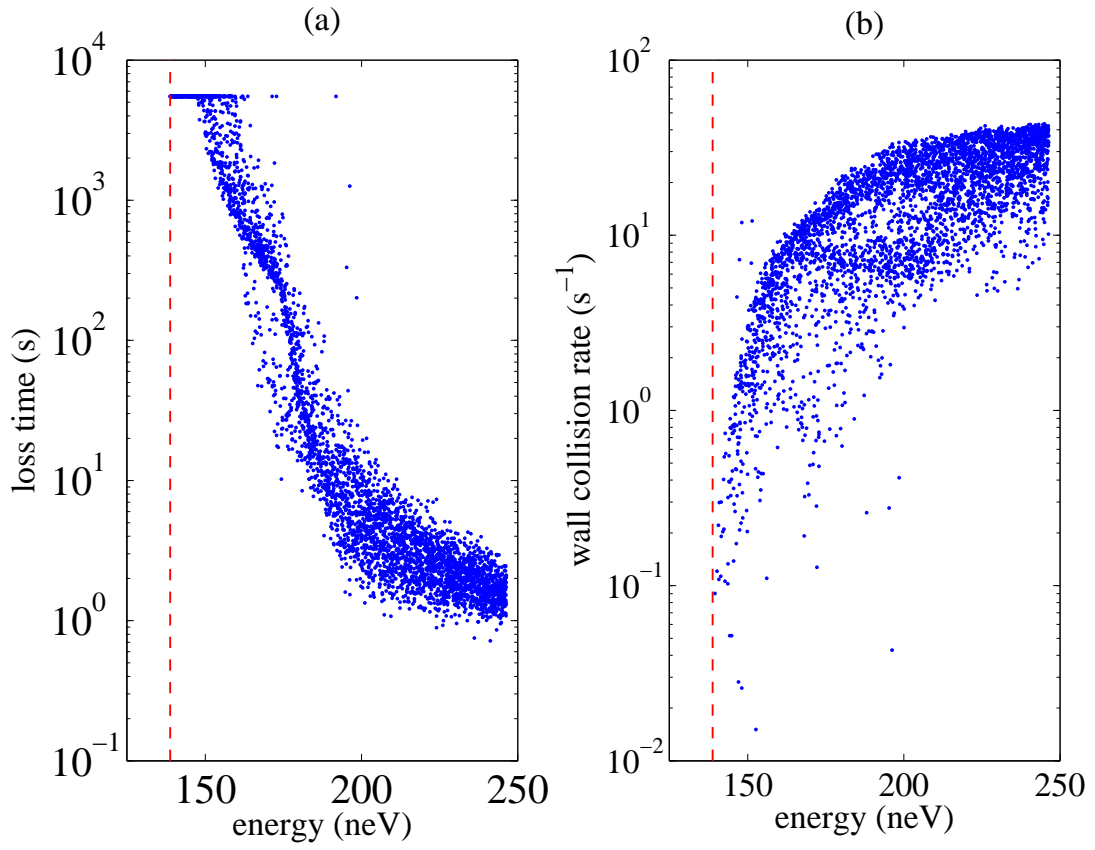


Figure 5: Loss time and wall collision rates³⁰ for simulated above threshold UCNs. A UCN is lost when its empirical survival probability falls below $1.0e-09$. Tracking halted 5500 s after creation time if a UCN has survival probability above $1.0e-09$.

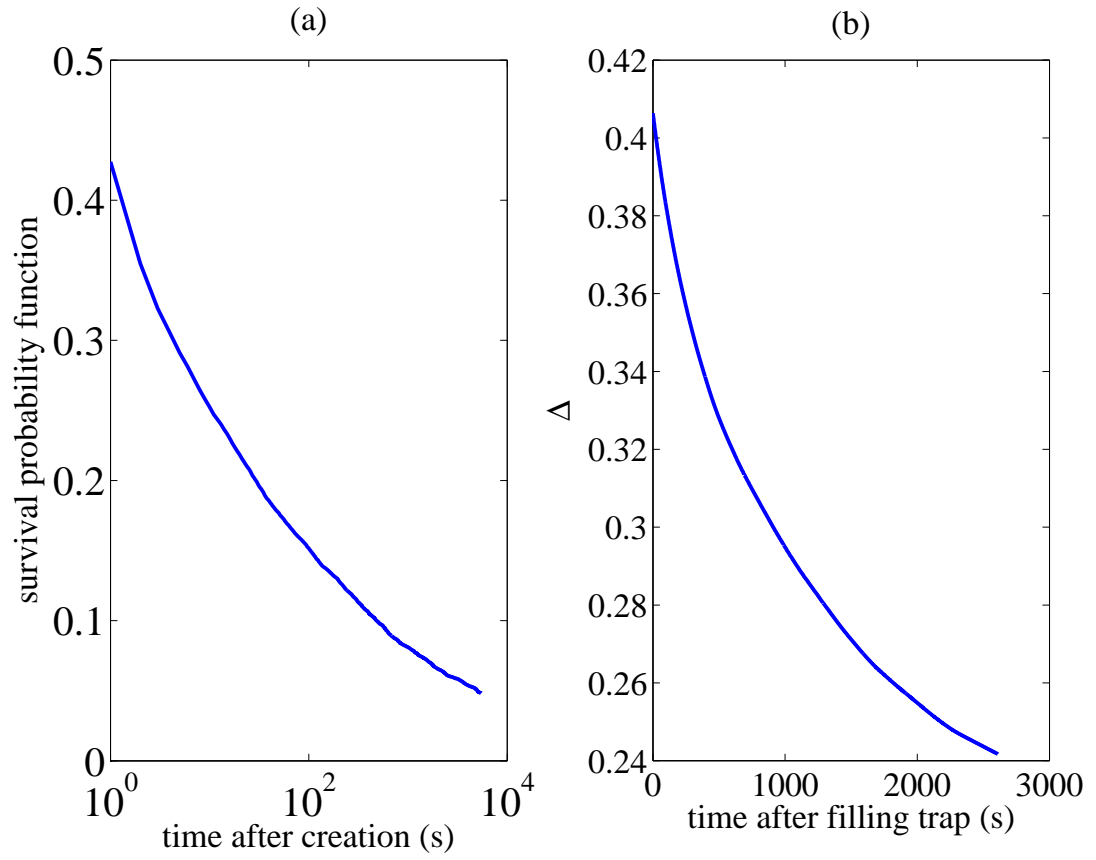


Figure 6: (a). Monte Carlo estimate of survival probability function of above threshold UCNs. (b). Monte Carlo estimate of distortion term $\Delta(t)$ (Eq. 16).

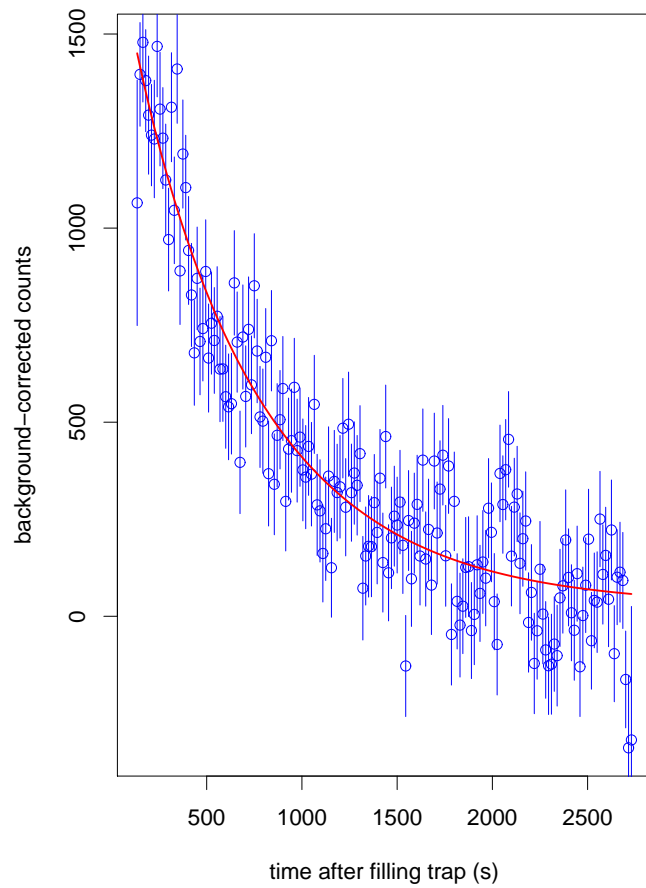


Figure 7: Observed and predicted (line) background-corrected data for a subset of data from the NIST magnetic trapping experiment. For this subset, the trapping potential is static. Prediction model accounts for wall losses.

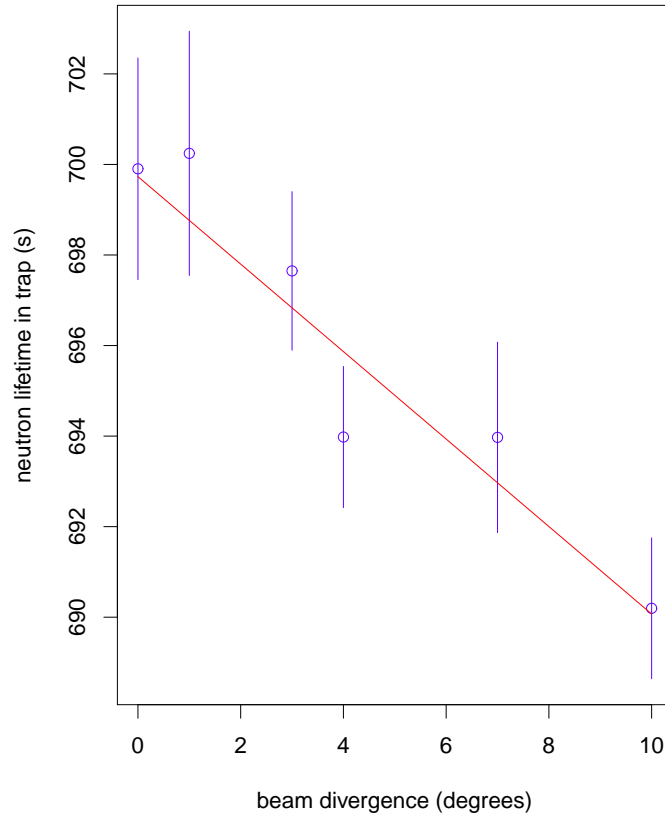


Figure 8: Model Carlo estimates of $\Delta(t)$ depend on assumed beam divergence within the trap. Fitted intercept and slope are $699.73(1.03)$ and $-0.97(0.17)$ s / degree.

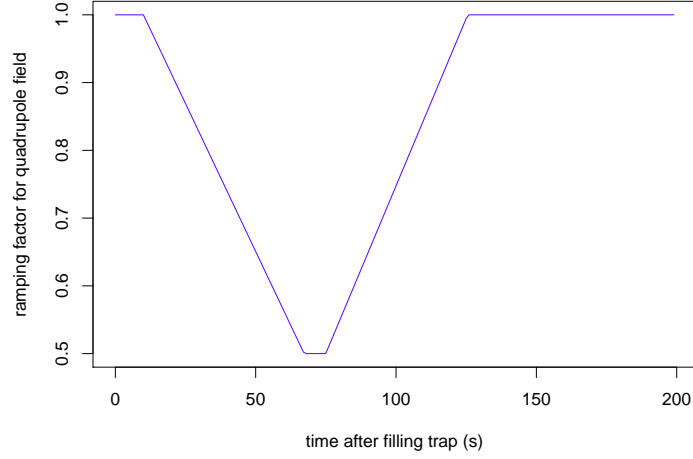


Figure 9: In simulation experiment, the quadrupole field is reduced by a fraction that varies from 1 to an adjustable minimum.

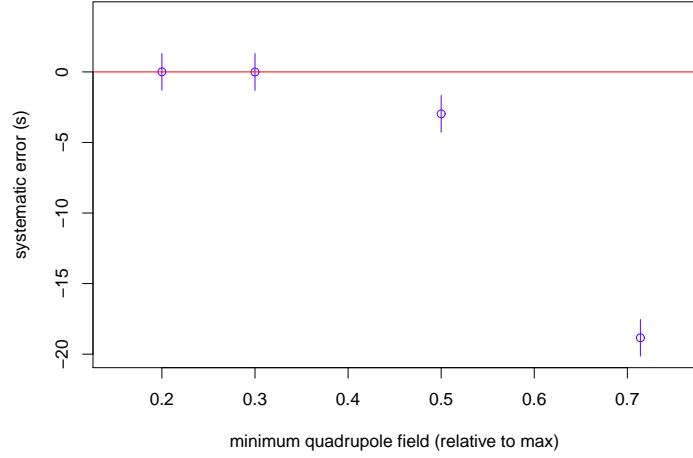


Figure 10: Bias of neutron lifetime when an exponential model is fit to simulated data contaminated by above threshold UCNs. For unramped field, bias is $-31(2)$ s. The true value of τ_* is 686 s.